Applied Surface Science 627 (2023) 157276

Contents lists available at ScienceDirect

Applied Surface Science

journal homepage: www.elsevier.com/locate/apsusc

Full Length Article

Laser-assisted two-step glass wafer metallization: An experimental procedure to improve compatibility between glass and metallic films

Albin Antony [a], Michal Hejduk [a,*], Tomáš Hrbek [a], Peter Kúš [a], Radka Bičišťová [b], Petr Hauschwitz [b], Ladislav Cvrček [c]

[a] Department of Surface and Plasma Science, Faculty of Mathematics and Physics, Charles University, V Holešovičkách 2, 180 00 Praha 8, Czech Republic
[b] Hilase Centre, Institute of Physics, Academy of Sciences of the Czech Republic, Za Radnicí 828, Dolní Břežany 25241, Czech Republic
[c] Department of Materials Engineering, Faculty of Mechanical Engineering, Czech Technical University in Prague, Karlovo náměstí 293/13, 120 00 Praha 2, Czech Republic

ARTICLE INFO

Keywords:
Glass
Glass metallization
Laser treatment
Surface adhesion
Microstructure

ABSTRACT

We report a simple and efficient two-step experimental procedure of glass metallization using laser microstructuring at ambient conditions. An adhesive pattern was created on the glass substrate using a laser, which imposes mechanical interlocking. An adhesive Cu layer was deposited on the glass substrate by magnetron sputtering and then electroplated with a functional Cu layer. Due to the unique surface structure created on the glass using laser, we achieved a thick layer of Cu metal film with high adhesion strength, well-defined grains and grain boundaries, and low surface roughness. The total thickness of the grown film was 11.4 μm, with an average surface roughness of 1.2 μm. The magnetron-sputtered coating did not show delamination from the glass substrate at a critical load of 60 N. The proposed method of glass metallization will lead to the realization of glass-based circuit materials that can be used in high-frequency electronic devices. Also, this procedure will be an alternative to chemical-based copper plating, which involves multiple processing steps and high-cost chemicals.

1 Introduction

Due to the increased data transmission rate, we are approaching the physical limitations of traditional PCB dielectric materials for electrical circuits under which electromagnetic compatibility can be controlled. The scientific community and industry are moving in search of new materials with features suitable for high-density circuitry, such as low thermal expansion coefficient (CTE), high dimensional stability, high thermal conductivity, and suitable dielectric constant [1]. Glass wafer offers several advantages in this regard, including that it is very stable in terms of electrical properties, moisture absorption, and aging, and has a CTE similar to that of silicon [2]. Furthermore, the low dielectric constant of glass coupled with a low loss tangent and low materials cost compared to high-performance materials make glass suitable for high-frequency applications [3,4]. Considering all these excellent properties, a perfect adhesion between metallic films and the glass substrate is the most important that needs to be satisfied for high-frequency device applications. The adhesion strength between the glass and metal is often inferior compared to metal-to-metal adhesion, and direct deposition of metallic film to glass substrate does not provide enough adhesion strength. Due to this, despite having excellent dielectric properties, the glass substrate is still not used in many high-frequency devices.

Commercially available high-frequency circuit materials exhibit a peel strength of 10 N/cm between the substrate material and metallic film [5]. To replace these materials with glass, it is important that glass wafers also should exhibit a peel strength in the same order of magnitude or more. Different approaches have been taken to overcome the adhesion issue between metallic film and glass [6–10]. The main difficulty in the realization of conductive plating of the glass substrate is the chemical and mechanical incompatibility between the glass and metallic films – that also holds for copper, the material most frequently used for circuit board manufacturing. The silicon oxide network of glass and the metallic network of Cu doesn't create a bond, resulting in poor adhesion [9]. Due to this structural incompatibility, chemical-based adhesion techniques involve multiple processing steps and expensive experimental procedures such as palladium activation [6], silanization [8],

* Corresponding author.
E-mail address: michal.hejduk@matfyz.cuni.cz (M. Hejduk).

https://doi.org/10.1016/j.apsusc.2023.157276
Received 7 January 2023; Received in revised form 15 March 2023; Accepted 12 April 2023
Available online 17 April 2023

and high-temperature annealing treatments [10]. It is worth noting that the adhesion strength shown by the glass wafers after chemical-based adhesion techniques is much lower than the (~1 N/cm) [8] commercially available high-frequency circuit materials (10 N/cm) [5].

In the present study, we report a novel method of glass metallization involving laser microstructuring and imposing mechanical-based adhesion. Smooth glass surfaces present no possibility of mechanical interlocking, so metal films can easily separate from the substrate. Laser-based microstructuring technique is categorized as a noncontact machining method and has been beneficial for glass materials, offering mask-less single-step processing capabilities [11–14]. Ultrashort (i.e., picosecond or femtosecond) pulsed lasers have shown great promise in high-precision glass machining with minimized heat-affected zone, thermal damage, and micro-cracks [15,16]. Using laser microstructuring, we create surface microstructures periodically distributed on the glass substrate [17], which serve as mechanical interlocking points and increase the adhesion between the glass substrate and film. Through the periodical structuring of glass, we can also control the glass wafer's surface roughness, which is considered one of the main disadvantages of mechanical-based adhesion. Once the surface modification is done, the treated glass substrate is deposited with a Cu adhesion layer via magnetron sputtering and then subjected to electroplating. While the last step is not required as the industrial magnetron sputtering devices can deposit several microns thick layers, it has the advantage that its deposition rate can be an order of magnitude higher than that of magnetron sputtering. The surface morphology and roughness of the films are studied using field emission scanning electron microscopy (FESEM) and atomic force microscopy (AFM). The adhesion strength is evaluated using a scratch tester. This direct method of glass metallization will be an alternative to chemical-based copper plating, which involves high-temperature annealing treatment [10], multi-layer deposition of metal oxides as adhesion promoters [6,8], multiple film deposition techniques [6,8–10] and high-cost palladium activation [6].

2 Experimental Procedure:

Fig. 1 shows the flow chart of the experimental procedure we followed in the present study. The total experimental process is divided into three steps: laser microstructuring of the glass, adhesion layer deposition, and (optional) electroplating. The details of each procedure are as follows:

2.1 Laser microstructuring of the glass substrate

A Borofloat 33 glass substrate with a thickness of 500 μm was used in the present study. Except removing the obvious impurities by alcohol, no special cleaning procedure was carried out prior to laser treatment. To create periodically distributed adhesion-promoting structures on the glass substrate, samples were treated by Ytterbium-based diode-pumped solid-state laser system Perla 100 (HiLASE, Czech Republic) [18] emitting 1.7 ps pulses with M^2 of 1.15 and wavelength of 1030 nm. The laser system generates linearly polarized pulses with up to 1 mJ pulse energy with a repetition rate of 100 kHz. To deflect the beam over the sample, a scanning head IntelliScan 14 (Scanlab, Germany) with 100 mm F-theta lens has been used for the delivery of the focused laser beam with a spot size of 30 μm. The RTC 5 control board (Scanlab, Germany) was utilized for the synchronous control of the scan system and the laser. The beam could be displaced on a sample with a maximum scanning speed of 2 m/s. Fig. 2 shows the schematic diagram of the experimental setup used for laser microstructuring.

2.2 Deposition of the Cu adhesion layer

The laser treated glass was subjected to standard glass cleaning procedure using acetone, alcohol and ultrasonic cleaner, mainly to remove fats and glass debris. The samples were prepared in a Flexilab 3 laboratory coating system (HVM Plasma, Czechia). The system was equipped with three two-inch magnetrons and a rotary heated table. The first two magnetrons were powered by a PD500X3 DC power supply (Kurt J. Lesker Company, USA), and the third magnetron was not used. During all experiments, two magnetrons with Cu (99.999%) targets were used simultaneously. On each magnetron, the power 250 W was applied. The rotating table was not powered, and therefore the glass

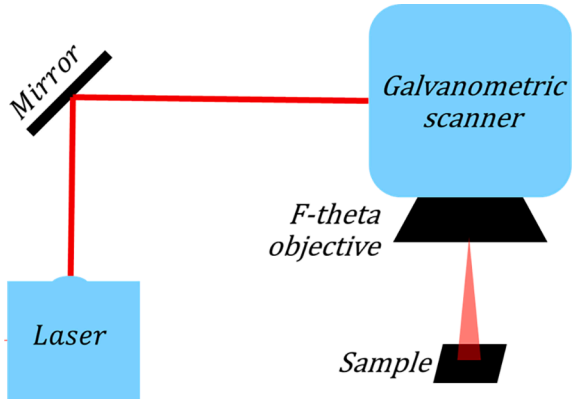

Fig. 2. Schematic diagram of the experimental setup used for laser microstructuring.

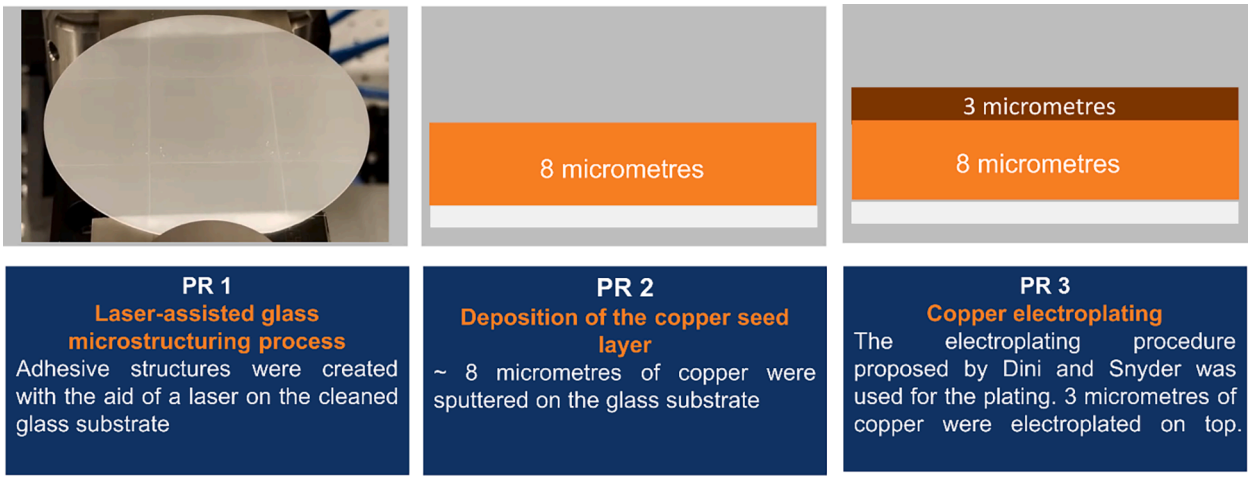

Fig. 1. Flow chart of the experimental procedures.

samples were on the floating potential. Next deposition parameters that were used: temperature 300 °C, time 1 h, pressure 0.8 Pa and Ar flow 20 sccm.

2.3 Electrodeposition of Cu.

The electroplating procedure proposed by Dini and Snyder is used in the present study [19]. The Cu bath solution is prepared using copper sulfate, sulphuric acid, and sodium chloride. The bath composition is 100 g/L $CuSO_4 \cdot 5H_2O$, 270 g/L H_2SO_4, and 0.1 g/L NaCl. A Cu foil is used as the anode. The distance between the anode and cathode is set at 10 cm. We pass a current of 6 mA/cm^2 for 5 min to achieve the obtained thickness of 3.4 μm of Cu film on top of the magnetron-sputtered layer.

2.4 Surface morphological and adhesion studies.

Adhesion tests were performed with the Revetest Scratch Xpress + scratch tester (CSM Instruments, Switzerland). A Rockwell diamond tip (radius 200 μm) was used as indentor. The scratch test load was set to increase linearly from 1 N to 100 N along the 10 mm scratch path with a linear speed of 10 mm/min. The surface morphology of the films was analyzed using FESEM at 10 kV accelerating voltage, and the images were captured at different view fields. The average surface roughness of the films on both the patterned glass wafer and Cu-plated glass wafer is estimated and studied using an atomic force microscope in tapping mode configuration.

3 Result and discussion

3.1 Laser microstructuring of glass

The interaction between a laser beam and the glass is determined by the wavelength emitted by the laser, its fluence, the pulse duration, repetition rate, pulse energy, and the material's physical and chemical properties [20]. The laser microstructuring procedure can increase the surface roughness of the glass as we remove the material from the polished surface. For high-frequency device applications, it is essential that we need to keep the average surface roughness of the glass wafer with Cu metal film lower than the skin effect depth to avoid the loss of signals [21]. Using laser-assisted microstructuring, we can control the experimental conditions for material ablation from the surface. Under the right ablation conditions, sites with a well-defined ablation depth arranged in predetermined geometric patterns are generated, shown in Fig. 3 (a) and 2(b). The pattern defines the ablation site density (the surface density of anchoring points for the conductive layer), which we demand to be as high as possible to increase the overall adhesion strength while avoiding the occurrence of microcracks due to excessive thermomechanical stress (shown in Fig. 3 (c)). In the present study, the periodic and highly precise patterning of the glass surface offered by the laser microstructuring has the potential to keep the average surface roughness of the wafer on the order of ~ 1 μm. This is comparable to the skin effect depth of the copper conductor (at frequency ~ 2 GHz) and will be able to decrease the scattering loss of signals in high-frequency device applications. The roughness measurement is discussed in section 3.3.

Another parameter to watch in future applications is the robustness of the circuit material, which greatly depends on the wafer thickness. With the 500 μm thick wafer, we could observe the loss of stiffness while performing scratch tests (Section 3.4) if both sides are laser-treated. Further characterizations were not in the scope of our current work.

3.2 Optimization of laser microstructuring parameters

To create periodically distributed adhesion-promoting structures on the glass substrate, the laser parameters, pulse energy, and the number of pulses must be carefully adjusted to avoid glass cracking and thermal damage in the modified region. The mircostructuring optimization parameters mainly involve the type of pattern, hatching distance, and ablation depth. Both laser beam and microstructuring parameters must be carefully selected to avoid thermal damage, localized melting, glass cracking, and, most importantly, to improve the adhesion force.

Based on the initial test to find the optimal process window for glass patterning, we chose two patterns: a hexagonal lattice pattern and a cross-hatching pattern with different hatching distances. Both patterns were created at a hatching distance (HD) of ~ 30 μm and an ablation depth of ~ 5 μm. The hexagonal lattice pattern consisted of dots located at the corners and centers of a honeycomb lattice, with each dot created by a single shot of the laser. The cross-hatching pattern was generated by sputtering away lines with the laser beam shifted at a speed of 700 mm/s. The spot size of the laser was 30 μm, the pulse repetition rate was 100 kHz, and the spatial overlap between pulses was approximately 77%.

Fig. 4(a) and 4(b) show the optical profilometer image of the pattern created. From the adhesion force test conducted between these two patterns, we found that hexagonal lattice patterns fail to hold the coating shown in Fig. 4(c), whereas cross-hatching patterns show excellent adhesion force. Further, to make the studies of pattern features complete, we reduce the HD of cross-hatching patterns to 15 μm and 10 μm and reduce the ablation depth to 2 μm. From the optical profilometer image shown in Fig. 4(d), the reduction in the HD results in the development of thermal damage and microcracks in the glass wafer. Hence, we settled on cross-hatching patterns with an HD of 30 μm and an ablation depth of ~ 5 μm. Fig. 4(e) shows the optical profilometer plot of the HD and ablation depth characteristics of the cross-hatching pattern made on the glass substrate. Fig. 4(f) and 4(g) show the image of the

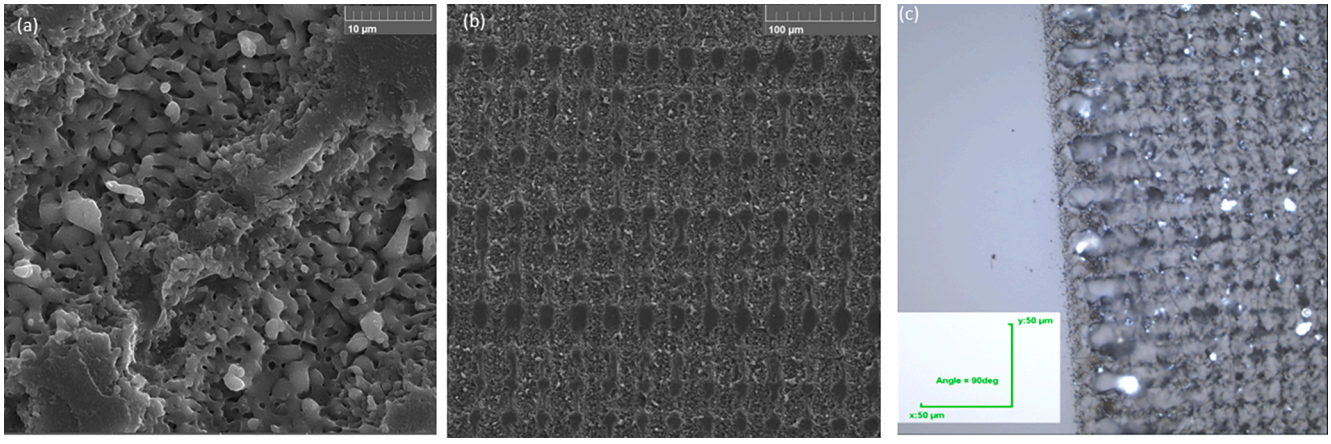

Fig. 3. (a) SEM image of the ablation pattern with dense microstructures (b) SEM image of the glass wafer with highly ordered ablation pattern (c) Optical profilometer image of microcracks formed on the glass wafer due to thermomechanical stress at wrong laser micro structuring parameters.

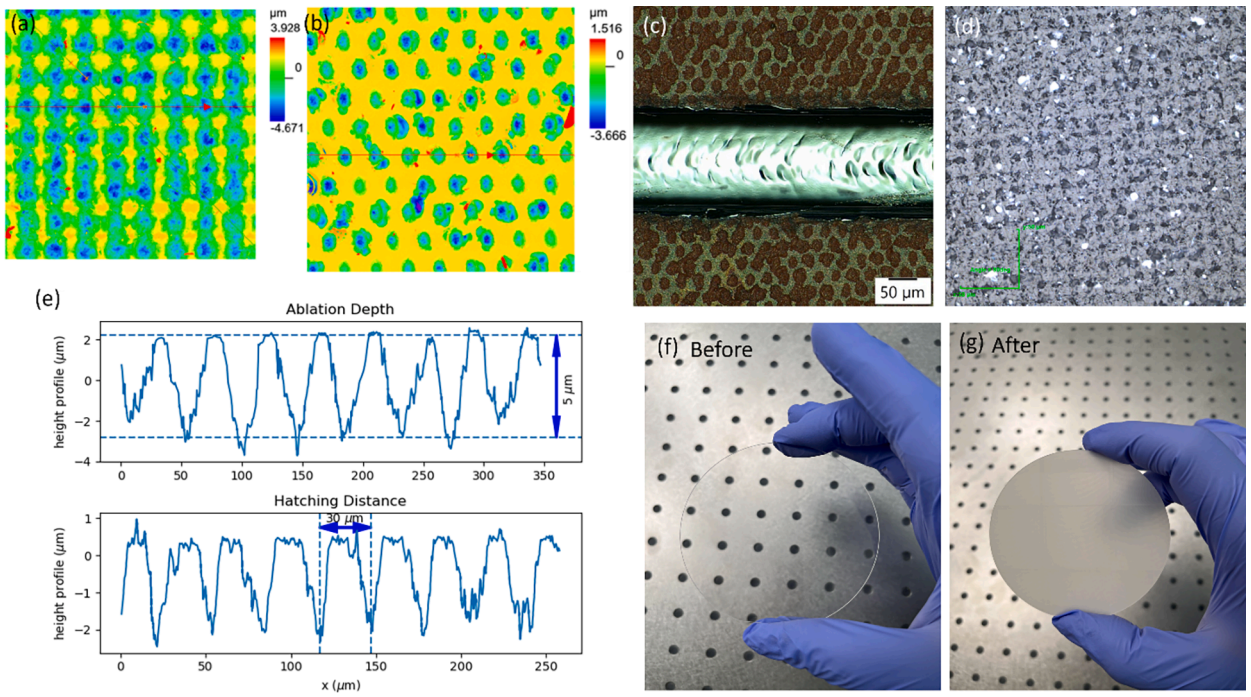

Fig. 4. (a) Optical profilometer image of the cross-hatching pattern (b) Optical profilometer image of the hexagonal lattice patterns created by laser microstructuring. (c) Adhesion force test evaluation on hexagonal lattice pattern conducted by scratch test (d) Optical microscope image of the microcracks formed on the glass wafer at 15 μm hatching distance (e) optical profilometer plot of the hatching distance and ablation depth evaluation on cross-hatching pattern (f) glass wafer image before microstructuring (g) glass wafer image after microstructuring.

glass wafers before and after laser microstructuring.

3.3 Morphology and roughness evaluation by SEM and AFM

The surface morphological features of the glass wafers after microstructuring is shown in Fig. 5(a). The SEM image reveals that patterns are made at a high order of precision, and the distance between each pattern is around ~ 30 μm which is in line with the laser profilometer measurement. Close inspection of the SEM image shows that the cross-hatching pattern results in the formation of well-defined pores and cavities, increasing the total contact area of the surface. From the cross-section view of the pattern shown in 5(b), the ablation depth is around 5 μm which is also in line with laser profilometer measurements. Fig. 5(c) and 5(d) show the image of copper-plated glass wafers. As evident from the SEM analysis, the growth of the copper layer on the patterned glass was highly uniform, with well-defined grains and grain boundaries. The plating of the copper was observed to be highly consistent, covering all the pores and cavities formed by the machining process. The proper covering of the surface irregularities formed by the microstructuring will result in mechanical interlocking, which eventually increases adhesive bond strength between the copper atoms and the oxide network of the glass wafers. Using the cross-section SEM analysis shown in Fig. 5(e), we calculated the total thickness of the plated copper and found it to be 11.4 μm. The exact figure shows that the vertical structure of the metal layer is the same everywhere regardless of the structure of the substrate.

The average surface roughness of the glass wafers was investigated by atomic force microscopy in tapping mode configuration. In high-frequency electronic devices, surface roughness in the order of skin effect depth of the conductor will lead to loss of signals through scattering [21,22]. Hence, keeping the average surface roughness of the Cu-glass wafer below the skin effect depth is crucial. Fig. 5(f) and 5(g) show the AFM image of the micromachined glass wafer before and after copper electroplating. We calculated the surface roughness of the laser micromachined glass wafer using Image J analysis software and found it to be 1.47 μm which is well within our experimental limit. Upon copper electroplating, the roughness values decreased to 1.2 μm, which signifies the uniform plating of copper on the surface irregularities created. We speculate that this kind of "smoothing" happens due to the preferential deposition of copper particles in laser-treated areas. The microstructures increase the density of sites where copper particles can bind – in stark contrast to the untreated (smooth) surface.

In conjunction with the vertical structure of the metal layer, as illustrated in Fig. 5(e), and its corresponding thickness, our measurements of the surface roughness strongly suggest that the electrical conductivity of the specimen remains uncompromised throughout. This conclusion is based on our observations of the surface roughness, which, while not direct evidence of conductivity, is nevertheless consistent with a uniform distribution of electrical conductivity on a scale of tens of microns.

3.4 Adhesion force evaluation by scratch tester

Initial tape adhesion tests showed that the hexagonal lattice pattern offers far weaker adhesion than the cross-hatching pattern, which can be associated with the lower density of laser-treated sites. Then, we performed a load-based scratch test to study the adhesion strength of the deposited copper with the glass [23]. The thickness of the Cu layer subjected to the tests presented here was 8 μm and it was reached by magnetron sputtering only. We conducted the test by linearly increasing the load from 0 to 100 N along a path of 10 mm with a loading speed of 10 mm/min (Fig. 6b). We found that the Cu-glass samples withstand a force of 60 N without delamination (Fig. 6a). Around the scratch there was only rolled up copper. The enhanced adhesion between the Cu film and glass substrate is mainly due to the mechanical interlocking mechanism. The cross-hatched surface patterns created via laser microstructuring resulted in surface irregularities on the smooth glass substrate. The Cu atoms deposited will penetrate the pores and cavities of the surface-modified glass substrate resulting in the mechanical interlocking between the glass surface and Cu atoms. This phenomenon contributes to improved adhesion. Apart from this, we assume that the

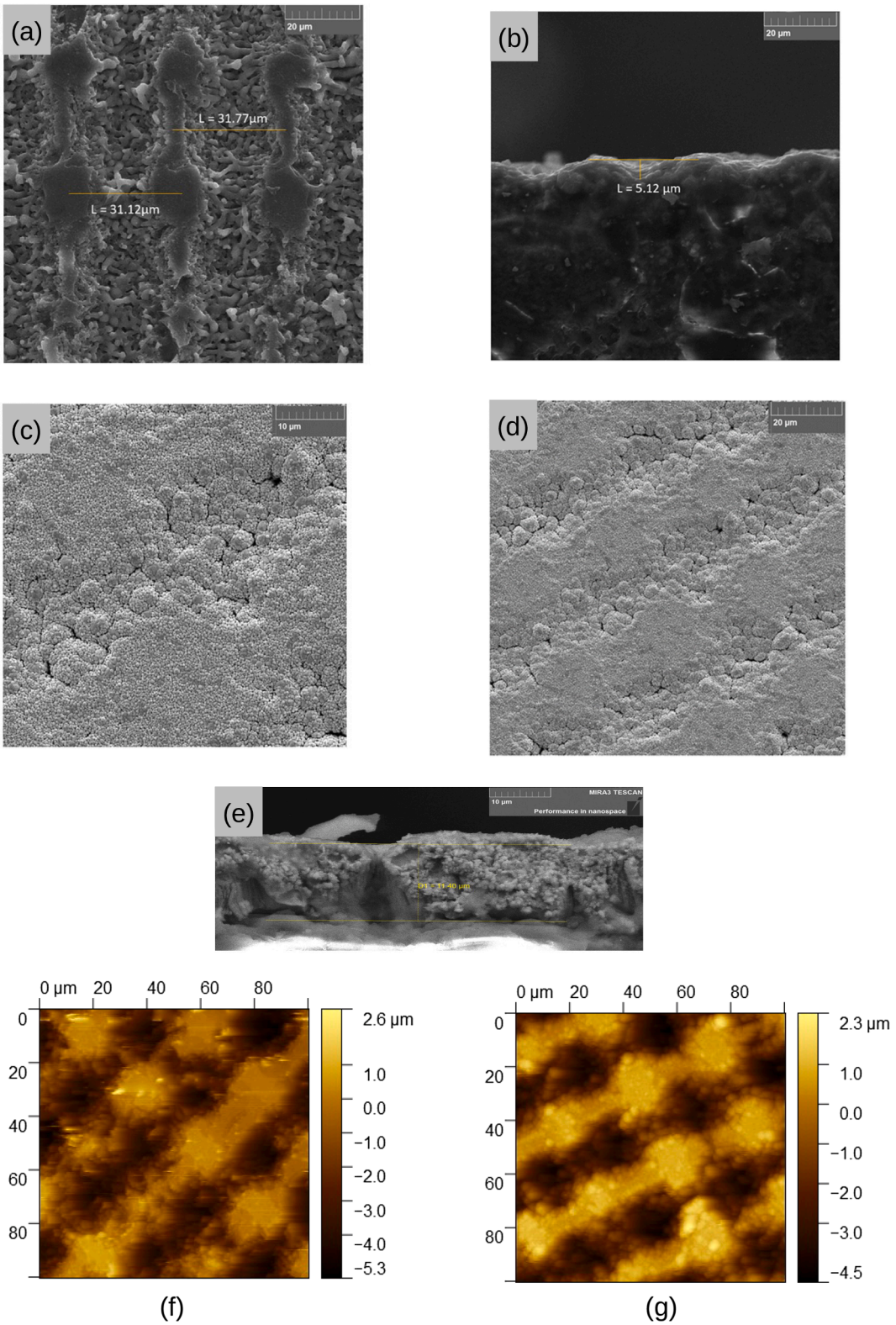

Fig. 5. (a) Surface morphological features of the glass wafers after microstructuring (b) Cross-section SEM view of the cross-hatching pattern (c) & (d) Morphology of copper-plated glass wafers on the patterns shown at different scan areas (e) Cross-sectional image of the plated copper on the glass with thickness scale (f) 2D AFM image of the micromachined glass wafer (g) 2D AFM image of the micromachined glass wafer with copper electroplated.

formation of a clean and highly reactive surface after laser patterning and an increase in a contact surface which increases the total contact area between the glass surface and Cu atoms will also contribute positively toward improved adhesion.

4 Conclusion

Laser-assisted glass microstructuring was performed to enhance the adhesion force between the glass and Cu metallic film. An adhesion

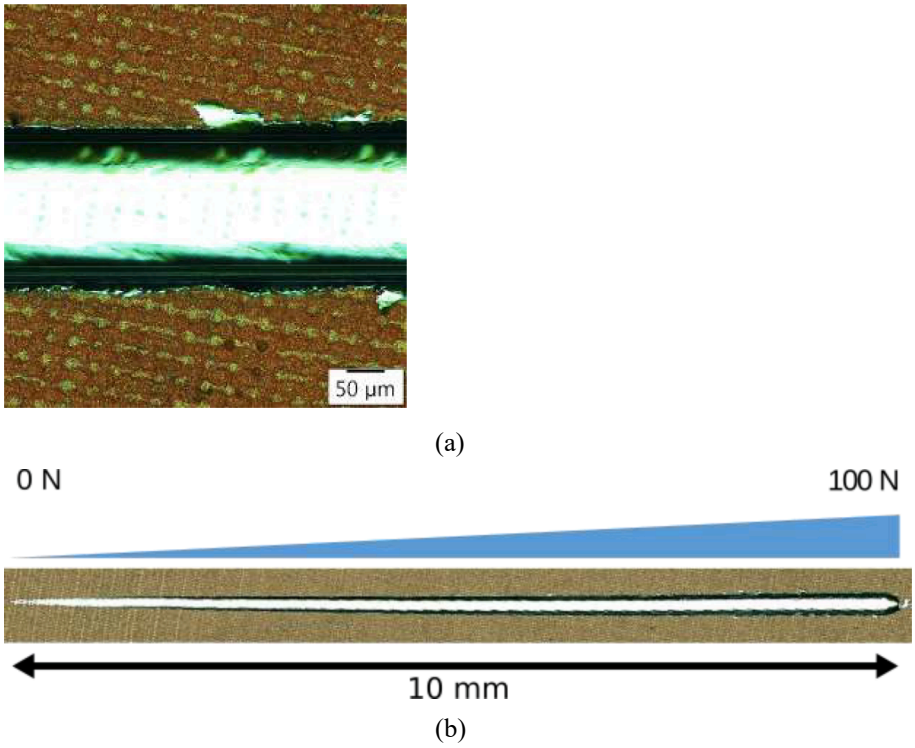

Fig. 6. (a) Optical microscope image of the copper-glass wafer with scratch at 60 N, (b) Optical microscope image of the scratch created on the glass wafer.

pattern called cross-hatching was derived using the picosecond laser pulse based on multiple optimization studies. Using laser micro-structuring, cross-hatching patterns were created on the glass substrate with high-order precision without thermal damage and microcracks. A 8 µm thick Cu adhesion layer was deposited on the treated wafer by sputtering, and then the wafer was subjected to an electroplating procedure to obtain the desired level of thickness. Using the FESEM technique, the surface morphology of the laser micromachined glass wafer and Cu- glass wafers were analyzed. The FESEM analysis shows that the laser microstructuring results in the formation of well-defined pores and cavities. The growth of the copper layer on the patterned glass was highly uniform, with well-defined grains and grain boundaries. A total thickness of 11.4 µm of Cu layer was calculated using cross-sectional FESEM analysis. The average surface roughness of the glass wafers was evaluated using AFM analysis and found to be 1.4 µm reduced to 1.2 µm upon copper electroplating. The adhesion strength of Cu with glass wafers was studied using a scratch test. The Cu-glass wafer exhibits excellent strength with an adhesion force of 60 N. The obtained features of the Cu-glass wafers, with their excellent adhesion strength and low roughness, make them an ideal candidate as a circuit material for next-generation high-frequency electronic devices. Further, the reported simple and efficient glass metallization procedure is an alternate method to the highly complex and costly chemical-based glass metallization procedure.

CRediT authorship contribution statement

Albin Antony: Methodology, Investigation, Visualization, Writing – original draft. **Michal Hejduk:** Conceptualization, Investigation, Resources, Writing – review & editing, Project administration, Funding acquisition. **Tomáš Hrbek:** Investigation. **Peter Kúš:** Investigation, Resources. **Radka Bičišťová:** Investigation. **Petr Hauschwitz:** Methodology, Investigation, Resources. **Ladislav Cvrček:** Methodology, Investigation, Resources.

Declaration of Competing Interest

The authors declare that they have no known competing financial interests or personal relationships that could have appeared to influence the work reported in this paper.

Data availability

Data will be made available on request.

Acknowledgement

We would like to thank Daniil Nikitin from the Department of Macromolecular Physics (Faculty of Mathematics and Physics, Charles University) for providing access to the atomic force microscope. This project was supported by the Primus Research Programme (Project Id. PRIMUS/21/SCI/005) of Charles University, the European Regional Development Fund and the state budget of the Czech Republic (project HiLASE CoE: Grant No. CZ.02.1.01/0.0/0.0/15_006/0000674).

References

[1] R. R. Tummala, "Moore's Law for Packaging to Replace Moore's Law for ICS," 2019 Pan Pacific Microelectronics Symposium (Pan Pacific), 1-6 (2019), doi: https://doi.org/10.23919/PanPacific.2019.8696409.
[2] S. Sivapurapu , R. Chen , M. ur Rehman, K. Kanno, T. Kakutani , M. Letz , F. Liu , S. K. Sitaraman , M. Swaminathan, Flexible and Ultra-Thin Glass Substrates for RF Applications, 2021 IEEE 71st Electronic Components and Technology Conference (ECTC), 1638-1644, (2021) doi: https://doi.org/10.1109/ECTC32696.2021.00260.
[3] S.M. Garner, S.C. Lewis, D.Q. Chowdhury, Flexible glass and its application for electronic devices, 2017 24th International Workshop on Active-Matrix Flat panel Displays and Devices (AM-FPD), 28-33 (2017).
[4] X. Cui, D. Bhatt, F. Khoshnaw, D.A. Hutt, P.P. Conway, Glass as a Substrate for High Density Electrical Interconnect, 2008 10th Electronics Packaging Technology Conference, 12-17, (2008) doi: https://doi.org/10.1109/EPTC.2008.4763405.
[5] Rogers Corporation, 2022, RO4000® Series High-Frequency Circuit Materials, Rogers Corporation, 21/10/2022, https://www.rogerscorp.com/advanced-electronics-solutions/ro4000-series-laminates/ro4003c-laminates.

[6] C.E.J. Cordonier, K. Okabe, Y. Horiuchi, A. Nakamura, K. Ishikawa, S. Seino, S. Takagi, H. Honma, Langmuir 33 (2015) 14571–14579, https://doi.org/10.1021/acs.langmuir.7b03329.
[7] G.E. Granados, L. Lacroix, K. Medjaher, Condition monitoring and prediction of solution quality during a copper electroplating process, J. Intell. Manuf. 31 (2020) 285–300, https://doi.org/10.1007/s10845-018-1445-4.
[8] A. Miller, L. Yu, J. Blickensderfer, R. Akolkar, Electrochemical Copper Metallization of Glass Substrates Mediated by Solution-Phase Deposition of Adhesion-Promoting Layers, J. Elec. Chem. Soc. 162 (14) (2015) D630–D634, https://doi.org/10.1149/2.1071514jes.
[9] L. Wu, L. Meng, Y. Wang, S. Zhang, W. Bai, T. Ouyang, M. Lv, X. Zeng, Effects of laser surface modification on the adhesion strength and fracture mechanism of electroless-plated coating, Surf. Coat. Technol. 429 (2022), 127927, https://doi.org/10.1016/j.surfcoat.2021.127927.
[10] K. Okabe, T. Kagami, Y. Horiuchi, O. Takai, H. Honma, C.E.J. Cordonier, Copper Plating on Glass Using a Solution Processed Copper-Titanium Oxide Catalytic Adhesion Layer, J. Elec. Chem. Soc. 163 (5) (2016) D201–D205, https://doi.org/10.1149/2.0071606jes.
[11] K. Ratautasa, A. Jagminienėa, I. Stankevičienėa, E. Norkusa, G. Račiukaitis, Laser assisted fabrication of copper traces on dielectrics by electroless plating, Procedia CIRP 74 (2018) 367–1337, https://doi.org/10.1016/j.procir.2018.08.144.
[12] B. He, J. Petzing, P. Webb, R. Leach, Improving copper plating adhesion on glass using laser machining techniques and areal surface texture parameters, Opt. Lasers Eng. 75 (2015) 39–47, https://doi.org/10.1016/j.optlaseng.2015.06.004.
[13] Y. Wang, L. Shen, W. Jiang, X. Wang, M. Fan, Z. Tian, X. Han, Laser processing as an alternative electrodeposition pretreatment, Surf. Coat. Technol. 357 (2019) 957–964, https://doi.org/10.1016/j.surfcoat.2018.11.005.
[14] E.G. Baburaj, D. Starikov, J. Evans, G.A. Shafeev, A. Bensaoula, Enhancement of adhesive joint strength by laser surface modification, Int. J. Adhes. Adhes. 27 (2007) 268–276, https://doi.org/10.1016/j.ijadhadh.2006.05.004.
[15] Z. Wang, D. Nandyala, C.E. Colosqui, T. Cubaud, D.J. Hwang, Glass surface micromachining with simultaneous nanomaterial deposition by picosecond laser for wettability control, Appl. Surf. Sci. (546) 149050 (2021), https://doi.org/10.1016/j.apsusc.2021.149050.
[16] P. Hauschwitz, J. Brajer, D. Rostohar, J. Kopeček, T. Mocek, M. Cimrman, M. Chyla, M. Smrž, Anti-Reflection Nanostructures on Tempered Glass by Dynamic Beam Shaping, Micromachines 12 (3) (2021) 28, https://doi.org/10.3390/mi12030289.
[17] S. Xu, K. Sun, C. Yao, H. Liu, X. Miao, Y. Jiang, H. Wang, X. Jiang, X. Yuan, X. Zu, Periodic surface structures on dielectrics upon femtosecond laser pulses irradiation, Opt. Express 27 (2019) 8983–8993, https://doi.org/10.1364/OE.27.008983.
[18] M. Smrž, J. Mužík, D. Štěpánková, H. Turčičová, O. Novák, M. Chyla, P. Hauschwitz, J. Brajer, J. Kubát, F. Todorov, Picosecond thin-disk laser platform PERLA for multi-beam micromachining, OSA Continuum 4 (3) (2021) 940–952, https://doi.org/10.1364/OSAC.418293.
[19] J.W. Dini, D.D. Snyder, Electrodeposition of copper, in: Modern Electroplating, Hoboken, NJ, USA:Wiley, (47) 33-78, 2011. https://doi.org/10.1002/9780470602638.ch2.
[20] A. Piqud, D.B. Chrisey, C.P. Christensen, Laser Direct-Write Micromachining, in: Direct-Write Technologies for Rapid Pro to typing Applications, Academic Press, Washington, D.C., USA, 2002, pp. 385–412.
[21] S. De, A.Y. Gafarov, M.Y. Koledintseva, R.J. Stanley, J.L. Drewniak, S. Hinaga, Semi-automatic copper foil surface roughness detection from PCB microsection images, Proc. Int. IEEESymp. Electromag. Compat, Pittsburgh, PA, 2012, pp. 5–10.
[22] M.Y. Koledintseva, A.G. Razmadze, A.Y. Gafarov, Soumya De, J.L. Drewniak, S. Hinaga, PCB Coductor Surface Roughness as a Layer with Effective Material Parameters, Proc. of IEEE EMC Symposium, 138-143, (2012).
[23] Y.M. Choi, D. Kang, J.N. Kim, I.K. Park, Evaluation of adhesion properties of thin film structure through surface acoustic wave dispersion simulation, Materials 15 (2022) 5637, https://doi.org/10.3390/ma15165637.